

Wavelength-stable cyan and green light emitting diodes on nonpolar *m*-plane GaN bulk substrates

Theeradetch Detchprohm,^{1,a)} Mingwei Zhu,¹ Yufeng Li,¹ Liang Zhao,¹ Shi You,¹ Christian Wetzel,¹ Edward A. Preble,² Tanya Paskova,² and Drew Hanser^{2,b)}

¹Department of Physics, Applied Physics, and Astronomy, and Future Chips Constellation, Rensselaer Polytechnic Institute, Troy, New York 12180, USA

²Kyma Technologies, Inc., 8829 Midway West Road, Raleigh, North Carolina 27617, USA

(Received 1 December 2009; accepted 6 January 2010; published online 1 February 2010)

We report the development of 480 nm cyan and 520 nm green light emitting diodes (LEDs) with a highly stable emission wavelength. The shift is less than 3 nm when the drive current density is changed from 0.1 to 38 A/cm². LEDs have been obtained in GaInN-based homoepitaxy on nonpolar *m*-plane GaN bulk substrates. For increasing emission wavelength we find a large number of additional dislocations generated within the quantum wells (2×10^8 to $\sim 10^{10}$ cm⁻²) and a decrease in the electroluminescence efficiency. This suggests that the strain induced generation of defects plays a significant role in the performance limitations. © 2010 American Institute of Physics. [doi:10.1063/1.3299257]

Current commercial high-efficiency white light emitting diodes (LEDs) combine a blue LED with a yellow phosphor. This provides record high luminous efficacy of 249 lm/W yet only at low current density (20 mA in 1 mm² devices) and with poor color rendering.¹ At typical currents of 350 mA, 161 lm/W has been reached.² To improve efficiency and color rendering, we pursue the direct emission approach combining red, green, and blue LEDs. This can theoretically provide an efficiency as high as 347 lm/W with high color-rendering index of 91.³ However, comparing light output power (LOP), green emitters are not yet at a level to match up with red and blue. This could be due to a large Stokes shift induced by the piezoelectric dipole across the GaInN/GaN quantum wells (QWs) in the polar *c*-plane growth. This polarization effect can be avoided via an epitaxial growth of the QWs along crystallographic directions with lower piezoelectric polarization, such as $[11\bar{2}4]$, or with vanishing polarization such as $[10\bar{1}0]$ *m*-axis and $[11\bar{2}0]$ *a*-axis.⁴ Several heteroepitaxial approaches implement such growth orientations^{5,6} yet, result in very high densities of threading dislocations (TDs) ($\sim 10^{10}$ cm⁻²) and stacking faults ($\sim 10^5$ cm⁻¹) likely limiting LED performance.⁶

The use of low-dislocation-density bulk GaN substrates sliced from boules recently resulted in better nonpolar homoepitaxial growth.^{7,8} UV and blue GaInN LEDs on the *m*-plane^{7,9,10} and green and yellow LEDs on semipolar $(11\bar{2}2)$ substrate,¹¹ have been demonstrated, the best of which show properties superior to those of *c*-plane growth.^{8–11}

In absence of the piezoelectric Stokes shift, a higher InN-fraction or a larger QW width than in *c*-plane growth is required to achieve the same long wavelength of green.¹² Lin *et al.*¹³ reported electroluminescence (EL) of blue-green *m*-plane LEDs by increasing the QW thickness. We demonstrated emission wavelengths up to 580 nm (yellow) in

m-plane QW growth in photoluminescence (PL).¹⁴ Here we report on nonpolar *m*-plane cyan and green LEDs and correlate the wavelength dependence of the LED efficiencies with structural properties as observed in transmission electron microscopy.

m-plane GaN substrates, 500 μm in thickness and 5×10 mm² in size were cut from *c*-axis grown hydride vapor phase epitaxy GaN (0001) boules. In chemomechanical polishing, an atomically flat surface was achieved [roughness ≤ 0.5 nm root mean square (rms)] (miscut $< 0.2^\circ$ toward *a*-axis and $\leq 1^\circ$ toward the *+c*-axis). Low-pressure metalorganic vapor phase epitaxy was used for homoepitaxial *m*-axis growth of multiple quantum well (MQW) (sample A–C) and full LED (sample D–G) structures; 0.5 μm thick Si-doped n-GaN layer, 5 or 8 periods of 3.9–4.4 nm thick nominally undoped Ga_{1-x}In_xN QW layers, and 24–26 nm thick undoped GaN barriers as the active region. By a variation in growth temperature, the InN-fraction (*x*) was controlled as determined from high resolution x-ray diffraction scans of the $(10\bar{1}0)$ plane. The emission wavelength scaled with *x* from 480 nm (*x*=13%) to 520 nm (*x*=19%). Furthermore, with *x*=15%, $Z_w=4.8$ nm an emission wavelength of 512 nm was achieved (Sample G). Pseudomorphic growth resulting in anisotropic strain and a negligible shear module were assumed. Further details of the growth process and the determination of the alloy composition have been reported in Ref. 14. Data on samples are summarized in Table I. The surface roughness for the active region was 0.2–0.5 nm (rms) and increased with *x*. The active region was capped by a Mg-doped p-layer sequence of a 20 nm thick Al_{0.18}Ga_{0.82}N electron blocking layer, a 100 nm thick GaN layer, and 20 nm thick highly doped GaN contact layer.

Across the peak wavelength range from 450 to 520 nm, room temperature PL spectra of all nonpolar MQW samples show single-peak emission. For structures with peak emission wavelengths from 480 to 520 nm, the spectral intensity drops by one order of magnitude while the linewidths are 150 ± 10 meV [full width at half maximum (FWHM)]. For an estimate of the internal quantum efficiency (IQE), the PL intensity at room temperature was compared with that at

^{a)} Author to whom correspondence should be addressed. Electronic mail: detcht@rpi.edu.

^{b)} Current affiliation: SRI International, Largo, FL, U.S.A.

TABLE I. Summary of *m*-plane GaInN/GaN MQW and LED samples: x : InN-fraction in QW (+/-5%); Z_w : QW thickness (+/-5%); λ : peak wavelength in PL for MQW and dominant wavelength in EL for LED (with variation within wafer).

Sample ID	Type	x (%)	Z_w (nm)	λ (nm)
A	MQW	10.0	4.4	456 +/- 2
B	MQW	12.5	3.9	487 +/- 2
C	MQW	15.0	4.8	512 +/- 6
D	LED	16.3	4.2	483 +/- 1
E	LED	19.0	4.1	489 +/- 1
F	LED	17.1	4.2	492 +/- 1
G	LED	18.6	4.6	516 +/- 3

4.2 K. In order to maximize photo carrier capture into the QWs, photoexcitation was performed at 408 nm in the transparent spectral region of the GaN layers. Under the common assumption of negligible nonradiative recombination at low temperature, we derive upper estimate values of IQE. In the 450 nm MQW sample (sample A), we find a very high value of 66% at room temperature. For longer emission wavelength, values drop to 35% at 478 nm (sample B) and to 8% at 500 nm (sample C).

For EL measurement in the *m*-plane LEDs, indium contacts of 1 mm diameter were formed on top of the p-GaN contact layer. LOP was measured through the substrate and a sapphire sample holder placed before the 1-cm-diameter orifice of a calibrated detector. Measurements inside an integrating sphere typically result in two to three times higher LOP. We observe single peak emission in all samples (D–G) [Fig. 1(a)]. The linewidths (FWHM) are 143–158 meV (27–33 nm) and increase with emission wavelength. Partial LOP at current density of 12.6 A/cm² reaches 2 mW for 480–490 nm LEDs (samples D and E) [Fig. 1(b)]. It drops to 1 mW in the 494 nm LED (sample F) and then to <0.2 mW for an emission peak longer than 510 nm (sample G). This 95% drop in LOP between 485 and 520 nm LEDs roughly parallels the 90% drop seen in IQE. As a function of drive current up to 38 A/cm², the 489, 494, and 511 nm LEDs (samples E, F, and G) reach maximum LOPs of 4.5, 1.3, and 0.2 mW, respectively [Fig. 2(a)]. The 511 nm LED (sample

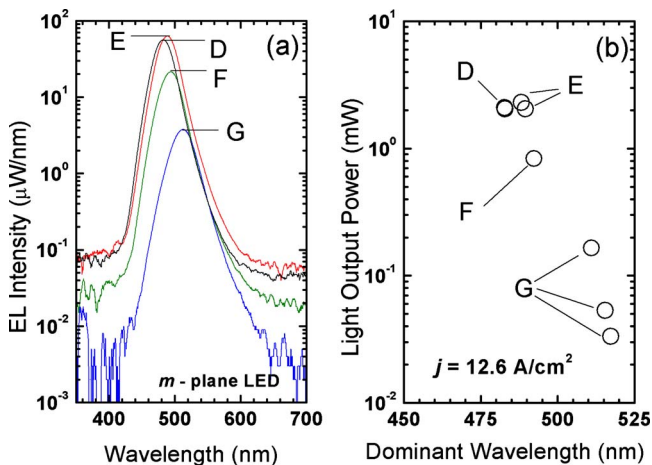


FIG. 1. (Color online) EL properties of *m*-plane cyan and green GaInN/GaN LEDs samples at 12.6 A/cm²: (a) emission spectra and (b) partial LOP as measured through the substrate. Emission wavelengths are very uniform within each sample except for sample G.

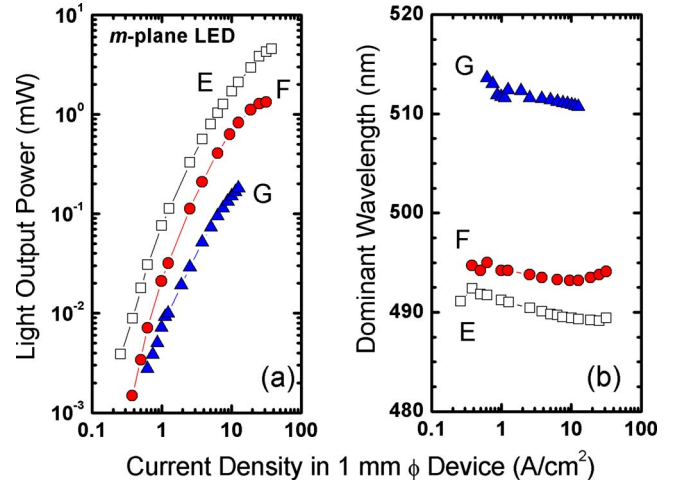


FIG. 2. (Color online) Current dependent EL characteristics of *m*-plane cyan and green GaInN/GaN LEDs: (a) partial LOP and (b) dominant wavelength.

G) shows a stronger efficiency droop than the shorter wavelength LEDs.

The emission wavelength as a function of drive current is shown in Fig. 2(b). Unlike polar *c*-plane LEDs, the dominant wavelength exhibits an extremely small shift of a mere 3 nm over the large current range of 0.3–38 A/cm². For comparison, blue shifts of 5 and 24 nm in dominant wavelength are typical in polar *c*-plane LEDs emitting at 484 and 510 nm, respectively. This blueshift is typically attributed to the partial screening of piezoelectric charges across the GaInN/GaN QWs which increase with InN fraction in polar *c*-plane LEDs. Here, however, we find evidence that such color shift in cyan and even green LEDs can be avoided with nonpolar *m*-plane growth.

In order to identify a possible reason for the efficiency decrease in the structures with increased emission wavelength, cross-sectional transmission electron microscopy (TEM) analysis was used to evaluate the crystallographic quality of LED samples across linear extensions of several micrometers. Data for the 483 nm cyan LED (sample D) is shown in Fig. 3(a). Apparently, all homoepitaxial layers are free from any additional TDs besides those protruding from the bulk substrate (nominally $<5 \times 10^6$ cm⁻²) and homoepitaxial n-GaN ($<1.7 \times 10^8$ cm⁻², our observation limit for this sample). However, in the 492 nm cyan LED (sample F, data not shown) there are a number of misfit dislocations (MDs) created in the QWs and these additional defects are found to propagate along the growth direction with an estimated density of $1-3 \times 10^8$ cm⁻². In a 516 nm green LED (sample G) [Fig. 3(b)] we derive a TD density as high as the

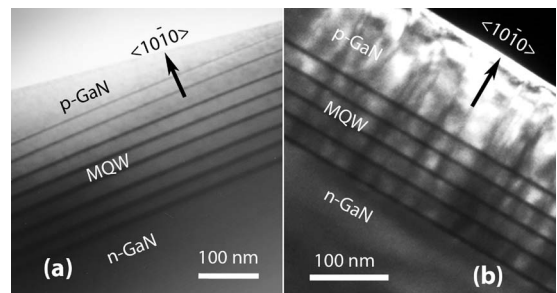


FIG. 3. Cross-sectional TEM micrographs of *m*-plane LEDs with dominant wavelength of (a) 483 nm (sample D), and (b) 516 nm (sample G).

upper 10^9 cm^{-2} to lower 10^{10} cm^{-2} within the active region and all subsequent layers. Using the invisibility criterion, where dislocations lose contrast under certain diffraction geometry, those TDs generated in the active region were found to be pure edge-type and to originate as MDs formed within the GaInN QW layers. This observation looks similar to our previously published finding in 532 nm polar *c*-plane LEDs grown on GaN bulk substrates, where TDs of similar concentration were found to originate in the GaInN QWs.¹⁵ Apparently, independently of the growth orientation, due to the large biaxial strain at the interface of GaN barriers and high InN-fraction GaInN wells, a high density of MDs is generated resulting in TDs. Those findings suggest that nonradiative recombination at the high density of TDs remains the most likely culprit in overall device performance limitations in the green spectral region.

In conclusion, we demonstrated the growth of *m*-plane LEDs with high InN-fraction GaInN/GaN MQWs for cyan and green (480–520 nm) LEDs by employing low-dislocation-density *m*-plane (100) GaN bulk substrates sliced from boules. With increasing emission wavelength we find a decreasing device performance that correlates with the generation of additional dislocations in the GaInN QWs as the InN-fraction increases. In absence of the piezoelectric polarization we find highly stable emission wavelengths under large variation of the drive current density. This aspect can be an important advantage for color reproducibility and color stability in high power all-color LEDs for energy-efficient solid-state lighting

This work was supported by a United States of America DOE/NETL Solid-State Lighting Contract of Directed Research under Grant No. DE-FC26-06NT42860. This work was supported by a United States of America DOE/NETL

Solid-State Lighting Contract of Directed Research under Grant No. DE-EE0000627. This work was also supported by the National Science Foundation (NSF) Smart Lighting Engineering Research Center (Grant No. EEC-0812056).

¹A. Michiue, T. Miyoshi, T. Yanamoto, T. Kozaki, S. Nagahama, Y. Narukawa, M. Sano, T. Yamada, and T. Mukai, *Proc. SPIE* **7216**, 72161Z (2009).

²Cree Inc, http://www.cree.com/press/press_detail.asp?i=1227101620851, November 19, 2008.

³Y. Ohno, *Proc. SPIE* **5530**, 88 (2004).

⁴T. Takeuchi, H. Amano, and I. Akasaki, *Jpn. J. Appl. Phys., Part 1* **39**, 413 (2000).

⁵T. Takeuchi, S. Lester, D. Basile, G. Girolami, R. Twist, F. Mertz, M. Wong, R. Schneider, H. Amano, and I. Akasaki, *IPAP Conf. Ser.* **1**, 137 (2000).

⁶A. Chakraborty, T. J. Baker, B. A. Haskell, F. Wu, J. S. Speck, S. P. DenBaars, S. Nakamura, and U. K. Mishra, *Jpn. J. Appl. Phys., Part 2* **44**, L945 (2005).

⁷A. Chakraborty, B. A. Haskell, S. Keller, J. S. Speck, S. P. DenBaars, S. Nakamura, and U. K. Mishra, *Jpn. J. Appl. Phys., Part 2* **44**, L173 (2005).

⁸T. Detchprohm, M. Zhu, Y. Li, Y. Xia, C. Wetzel, E. A. Preble, L. Liu, T. Paskova, and D. Hanser, *Appl. Phys. Lett.* **92**, 241109 (2008).

⁹M. C. Schmidt, K. C. Kim, H. Sato, N. Fellows, H. Masui, S. Nakamura, S. P. DenBaars, and J. S. Speck, *Jpn. J. Appl. Phys., Part 2* **46**, L126 (2007).

¹⁰K. Okamoto, H. Ohta, S. F. Chichibu, J. Ichihara, and H. Takasu, *Jpn. J. Appl. Phys., Part 2* **46**, L187 (2007).

¹¹M. Funato, M. Ueda, Y. Kawakami, Y. Narukawa, T. Kosugi, M. Takahashi, and T. Mukai, *Jpn. J. Appl. Phys., Part 2* **45**, L659 (2006).

¹²C. Wetzel, M. Zhu, J. Senawiratne, T. Detchprohm, P. D. Persans, L. Liu, E. A. Preble, and D. Hanser, *J. Cryst. Growth* **310**, 3987 (2008).

¹³Y. Lin, A. Chakraborty, S. Brinkley, H. C. Kuo, T. Melo, K. Fujito, J. S. Speck, S. P. DenBaars, and S. Nakamura, *Appl. Phys. Lett.* **94**, 261108 (2009).

¹⁴T. Detchprohm, M. Zhu, Y. Li, Y. Xia, L. Liu, D. Hanser, and C. Wetzel, *J. Cryst. Growth* **311**, 2937 (2009).

¹⁵M. Zhu, S. You, T. Detchprohm, T. Paskova, E. A. Preble, D. Hanser, and C. Wetzel (unpublished).